

**NASA
Technical
Memorandum**

NASA TM -86570

**EXPERIMENTAL EVALUATION OF THE RING FOCUS
TEST FOR X-RAY TELESCOPES USING AXAF'S
TECHNOLOGY MIRROR ASSEMBLY**

**MSFC Center Director's Discretionary Fund
Final Report, Project No. H20**

By D. E. Zissa and D. Korsch

**Information and Electronic Systems Laboratory
Science and Engineering Directorate**

October 1986

**(NASA-TM-86570) EXPERIMENTAL EVALUATION OF
THE RING FOCUS TEST FOR X-RAY TELESCOPES
USING AXAF'S TECHNOLOGY MIRROR ASSEMBLY,
MSFC CDDF PROJECT NO. H20 Final Report
(NASA) 15 p**

N87-15916

**Unclas
CSCL 03A G3/89 40318**



**National Aeronautics and
Space Administration**

George C. Marshall Space Flight Center

1. REPORT NO. NASA TM-86570		2. GOVERNMENT ACCESSION NO.		3. RECIPIENT'S CATALOG NO.	
4. TITLE AND SUBTITLE Experimental Evaluation of the Ring Focus Test for X-Ray Telescopes Using AXAF's Technology Mirror Assembly MSFC CDDF Final Report, Project No. H20				5. REPORT DATE October 1986	
				6. PERFORMING ORGANIZATION CODE	
7. AUTHOR(S) D. E. Zissa and D. Korsch				8. PERFORMING ORGANIZATION REPORT #	
9. PERFORMING ORGANIZATION NAME AND ADDRESS George C. Marshall Space Flight Center Marshall Space Flight Center, AL 35812				10. WORK UNIT, NO.	
				11. CONTRACT OR GRANT NO.	
12. SPONSORING AGENCY NAME AND ADDRESS National Aeronautics and Space Administration Washington, D.C. 20546				13. TYPE OF REPORT & PERIOD COVERED Technical Memorandum	
				14. SPONSORING AGENCY CODE	
15. SUPPLEMENTARY NOTES Prepared by Information and Electronic Systems Laboratory, Science and Engineering Directorate.					
16. ABSTRACT A test method particularly suited for x-ray telescopes was evaluated experimentally. The method makes use of a focused ring formed by an annular aperture when using a point source at a finite distance. This would supplement measurements of the best focus image which is blurred when the test source is at a finite distance. The telescope used was the Technology Mirror Assembly of the AXAF program. Observed ring image defects could be related to the azimuthal location of their sources in the telescope even though in this case the predicted sharp ring was obscured by scattering, finite source size, and residual figure errors.					
17. KEY WORDS ring focus, x-ray telescopes, optics, geometrical optics, AXAF, TMA, optical testing, x-ray testing, grazing incidence, grazing-incidence telescopes, x-rays			18. DISTRIBUTION STATEMENT Unclassified - Unlimited		
19. SECURITY CLASSIF. (of this report) Unclassified		20. SECURITY CLASSIF. (of this page) Unclassified		21. NO. OF PAGES 15	
				22. PRICE NTIS	

TABLE OF CONTENTS

	Page
INTRODUCTION	1
EXPERIMENTAL APPARATUS AND PROCEDURE	1
RESULTS.....	3
CONCLUSIONS	3
REFERENCES	5

PRECEDING PAGE BLANK NOT FILMED

LIST OF ILLUSTRATIONS

Figure	Title	Page
1.	Schematic of image space geometry where spherical aberration is due to a finite object distance	6
2.	Diagram of TMA optics	6
3.	Contour plot of ring image intensity data at predicted position of ring focus. One HRI pixel corresponds to 7.5 μm	7
4.	Radial profiles of ring annuli with 25 μm pinhole scan. Plot labels indicate distance in front of the best focus.....	8
5.	Variables used to describe correspondence between ring image and best focus image	9
6.	Parameterization of previously measured best focus image	10
7.	Model predictions from parameterized best focus data for radial profiles of ring annuli with a 25 μm pinhole scan. Plot labels indicate distance in front of the best focus	10

TECHNICAL MEMORANDUM

EXPERIMENTAL EVALUATION OF THE RING FOCUS TEST FOR X-RAY TELESCOPES USING AXAF'S TECHNOLOGY MIRROR ASSEMBLY

MSFC Center Director's Discretionary Fund Final Report,
Project No. H20

INTRODUCTION

If an axially symmetric system is illuminated by an on-axis point source through a narrow annular aperture, then, in the presence of spherical aberration, a sharply focused ring is formed in front of or behind the best-focus image plane, depending on the amount and the sign of the spherical aberration (Fig. 1). Any deviation from circular symmetry as well as changes in the thickness of the ring are indications of surface defects and alignment errors in the imaging system and may be analyzed as such. In an earlier paper [1] the test method [2] has been discussed theoretically for the telescope design of the Advanced X-ray Astrophysics Facility (AXAF) and results were given for a visible light test of a one-sixth scale model of the Hubble Space Telescope. The test method is only of limited value for visible light telescopes because widening of the ring due to diffraction with the larger wavelength through a narrow annular aperture tends to obscure the effect.

In this paper results are given from an experimental test of the method with the Technology Mirror Assembly (TMA) of the AXAF program. The TMA is roughly a two-thirds scale model of the smallest paraboloid-hyperboloid mirror pair planned for the AXAF program. The Marshall Space Flight Center (MSFC) test chamber and 1000-ft vacuum tunnel was used for the test.

EXPERIMENTAL APPARATUS AND PROCEDURE

The TMA is a Wolter Type 1 grazing-incidence telescope with one paraboloid-hyperboloid pair of mirrors (Fig. 2). Each element is roughly cylindrical with a 410 mm length. The elements are lined up along their axes with a 28 mm gap between them. The telescope has an entrance aperture diameter of about 427 mm and a nominal focal length of 6 m (the measured focal length was 5.97 m). The entrance annulus has a width of about 3.6 mm. The grazing angle of incidence is about 30 arcmin. The actual equations for the mirror surfaces derived from the specifications for the system are of the following form (Fig. 2):

$$h^2 - h_0^2 = 2kz - (1 + \delta) z^2$$

where:

$$h^2 = x^2 + y^2, \text{ where } x, y \text{ are transverse coordinates}$$

z = axis of symmetry

($z=0$ at center of each mirror, z is positive toward the front of each mirror)

$$h_0 = h \text{ at } z = 0$$

$$k = \text{subnormal at } z = 0$$

$$\delta = -e^2 \text{ where } e \text{ is the eccentricity}$$

$$d = 438 \text{ mm} = \text{distance between mirror centers}$$

(28 mm mirror gap midway between centers)

Paraboloid

$$h_{01} = 211.906860 \text{ mm}$$

$$k_1 = 1.836797 \text{ mm}$$

$$\delta_1 = -1.$$

Hyperboloid

$$h_{02} = 204.243289 \text{ mm}$$

$$k_2 = 5.377429 \text{ mm}$$

$$\delta_2 = -1.0006122657$$

For the 1000-ft source distance used here, the best focus was calculated to be 120 mm behind the infinite focus. The best focus was calculated to have a $13 \mu\text{m}$ rms diameter due to the finite source distance. The ring focus was predicted to be 41 mm in front of the best focus obtained with the 1000-ft source distance. It was calculated to have a diameter of 2.8 mm. The width of the focused ring geometrically would be $0.2 \mu\text{m}$ rms. However the source was effectively about 1 mm by $1/2 \text{ mm}$ or $20 \mu\text{m}$ by $10 \mu\text{m}$ at the ring focus and at the best focus. The diffraction width of the ring focus is about $3 \mu\text{m}$ between zeros of the sinc function for the x-ray wavelength of 8.34 \AA .

The TMA had already been placed in the test chamber of the 1000-ft vacuum tunnel at MSFC for tests at the best focus position. Cary Reily of the Test Laboratory had the facility readied for this experiment. X-rays of 8.34 \AA wavelength were used. The detectors were supplied by the Smithsonian Astrophysical Observatory (SAO) and were operated by Dan Schwartz of SAO. Dan Schwartz also supplied the data. One of the detectors was the High Resolution Imager (HRI) which is a microchannel plate detector with a resolution of about $30 \mu\text{m}$ and of a size that could image the whole ring. The other detector was a proportional counter with a $25 \mu\text{m}$ pinhole placed in front.

Data were taken at four positions in front of the overall best focus position. The best focus image had been measured by SAO in an earlier experiment in the same test chamber [3,4]. The four positions were 15.672, 28.372, 41.072, and 53.772 mm in front of the best focus with the 41.072 mm point being the predicted ring focus position. (The best focus position was experimentally determined by closing off all but one quadrant of the exit aperture at a time. The separate images produced by

this procedure were forced to overlap.) HRI data were taken at each axial position in order to see the overall ring. Then the 25 μm pinhole detector was scanned across the width of the ring at 12 μm intervals at the same orientation on each ring. The scan was made along the coordinate axis in which the source was narrower. The fact that the scan was actually made at a point on the ring 11 deg above the narrow axis has negligible effect here. The background rate was measured for the 25 μm pinhole scans.

RESULTS

First, an overall picture of the ring was obtained with the HRI detector with a resolution of 30 μm . A contour plot of these data at the predicted axial position of the ring focus is shown in Figure 3. This plot gives an idea of how uniform the ring was.

Figure 4 shows radial profiles of the ring annulus made with the 25 μm pinhole detector at intervals of 12 μm and integrated over 200 sec except for the 53.772 mm curve which was integrated for 100 sec and those counts were multiplied by two. Increasing values on the horizontal distance scale indicate motion from outside toward the inside of the annulus. Background counts of 62 per 200 sec integration time have been excluded from Figure 4. The widths of the profiles are all about 100 μm . The intensities decrease as the ring radius increases with distance in front of the best focus. Evidently the narrowing predicted for the ring focus has been obscured by scattering, the finite source size, and residual figure errors in the mirrors.

Since the best focus image had a full width at half maximum of about 14 μm [3] in the direction of the scan across the ring annulus, it seemed surprising at first that the ring distributions of Figure 4 were much wider and of constant width. This would not be the case if spherical aberration due to the finite source distance were the only image degrading cause. Since in this case scattering is predominantly responsible for the image spread, the appearance is quite explicable. The best focus is formed where the central ring of the annular image collapses to a point. Only at this location do the intensities from around the annulus overlap in a small area. Therefore, the intensity grows sharply towards the center of the best focus spot. To give a more quantitative explanation of the effect, a simple computer model was developed. Actually, the procedure was carried out in reverse by using previously measured best focus image data, and convolving the results with a 25 μm pinhole. In the notation of Figure 5, the energy in radial increment " dr " at radius " Δr " in the best focus image would be mapped in equal parts to radial increments " dr " at radii " $r_0 + \Delta r$ " and " $r_0 - \Delta r$ " in the annulus. For the best focus image distribution, a parameterization (Fig. 6) of the measured distribution was used from Reference 4. Even though that parameterization assumed circular symmetry, the results still should give some idea of what the ring data should look like. The results are shown in Figure 7. The shape, width, and relative intensities from the model are similar to those of the measured data shown in Figure 4.

CONCLUSIONS

The ring focus test method provides a most sensitive procedure to measure surface defects of telescopes, in particular grazing-incidence telescopes with narrow

entrance annuli. Since the width of the ring focus of a perfect telescope is (neglecting diffraction effects) generally small compared to the best focus image, errors can be detected that would normally be obscured by the presence of spherical aberration in the focal plane. To measure defects of this magnitude, however, requires an almost perfect optical system, and a source the ideal image of which should be small compared to the aberrations caused by the finite source distance. But even in the presence of a significant amount of near angle scattering, as in the present case, observations in the neighborhood of the ring focus can yield valuable information. By radially unfolding the best focus image into a ring pattern it becomes possible to relate an observed image defect to the azimuthal location of its source in the telescope. This information is obtained by carrying out radial scans at different azimuthal angles, whereby the theoretical image of the source should be small compared to the measured image spread, and preferably of circular shape. The measurements performed on the TMA and discussed here excellently demonstrate this property of the test.

REFERENCES

1. Griner, D. B., Zissa, D. E., and Korsch, D.: Test Method for Telescopes Using a Point Source at a Finite Distance. NASA Technical Memorandum 86523, Marshall Space Flight Center CDDF Project No. H20, September 1985.
2. Korsch, D.: Design and Analysis in Support of AXAF. Final Report to Marshall Space Flight Center, Contract NAS8-35622, April 1985.
3. Schwartz, D. A., et al.: X-ray Testing of the AXAF Technology Mirror Assembly (TMA) Mirror. In SPIE Proceedings "X-ray Instrumentation in Astronomy," J. L. Culhane, ed., Vol. 597, 1986, p. 10.
4. Van Speybroeck, L., et al.: Correspondence Between AXAF TMA X-ray Performance and Models Based upon Mechanical and Visible Light Measurements. In SPIE Proceedings "X-ray Instrumentation in Astronomy," J. L. Culhane, ed., Vol. 597, 1986, p. 20.

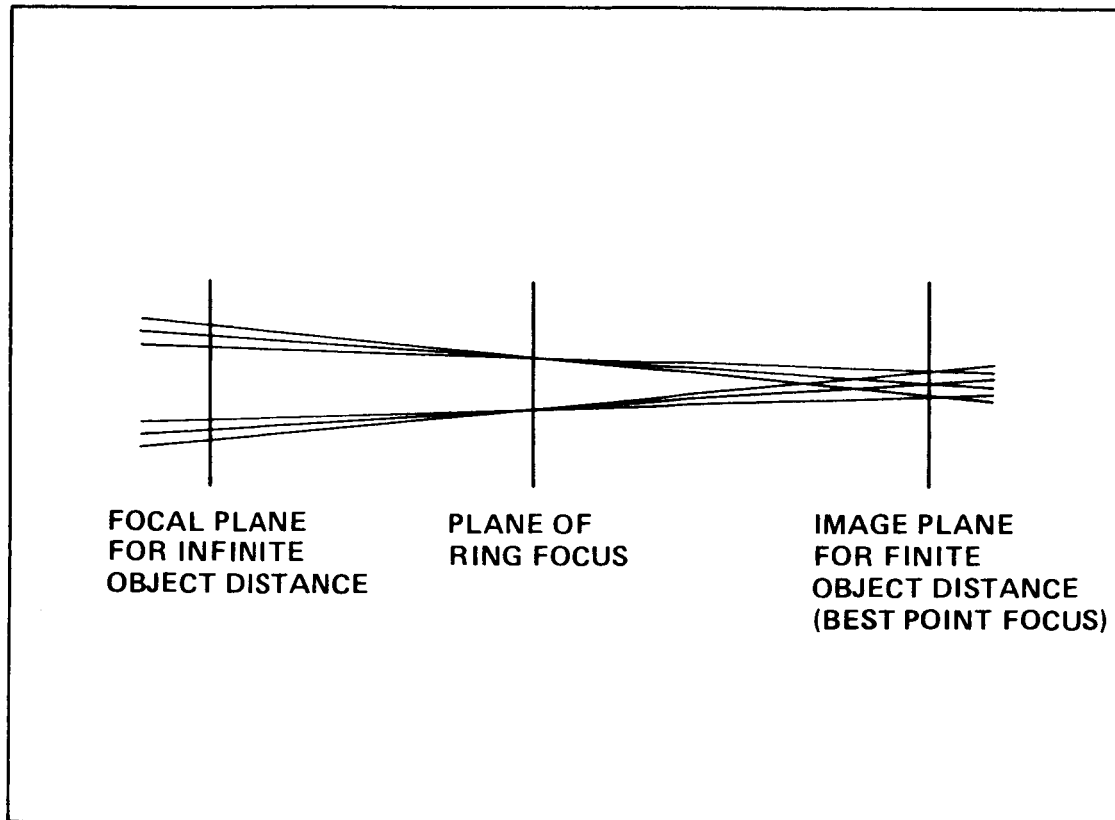


Figure 1. Schematic of image space geometry where spherical aberration is due to a finite object distance.

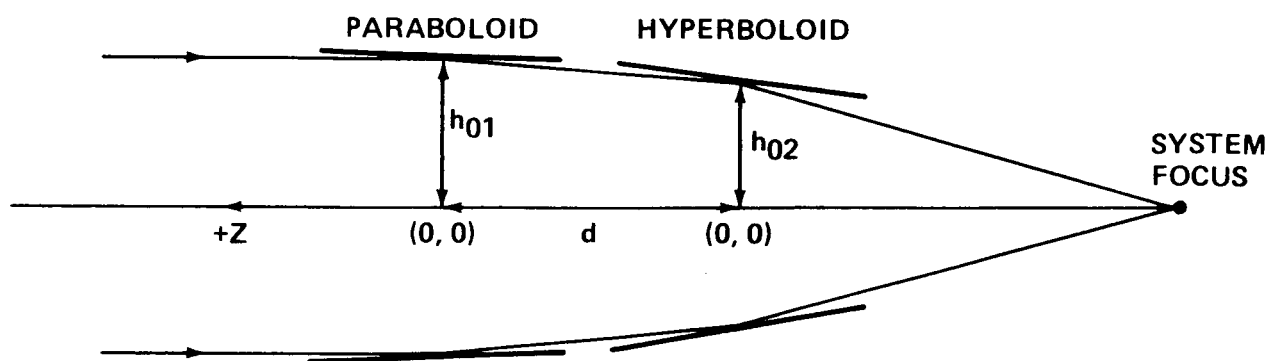


Figure 2. Diagram of TMA optics.

ORIGINAL PAGE IS
OF POOR QUALITY

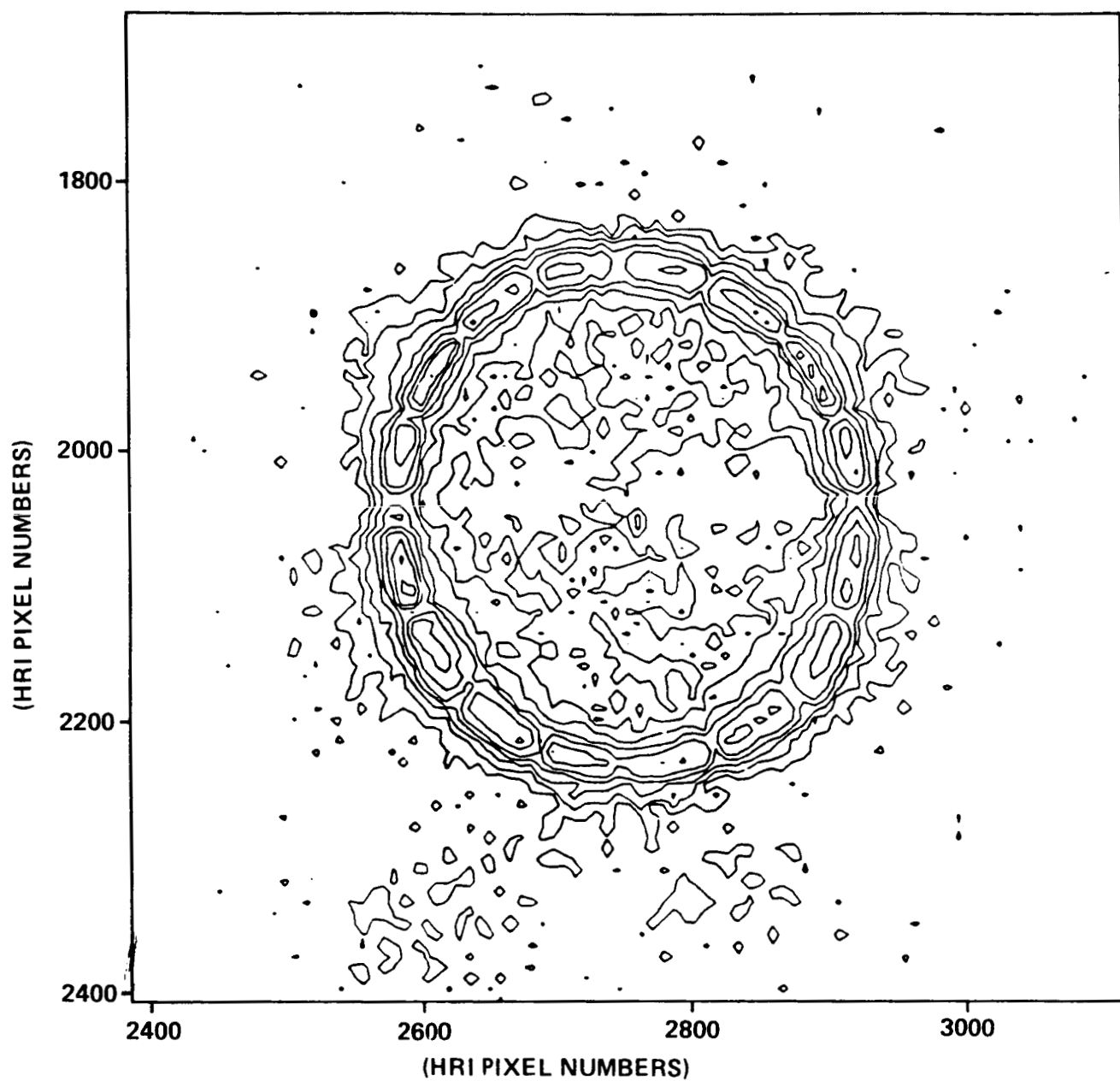


Figure 3. Contour plot of ring image intensity data at predicted position of ring focus. One HRI pixel corresponds to $7.5 \mu\text{m}$.

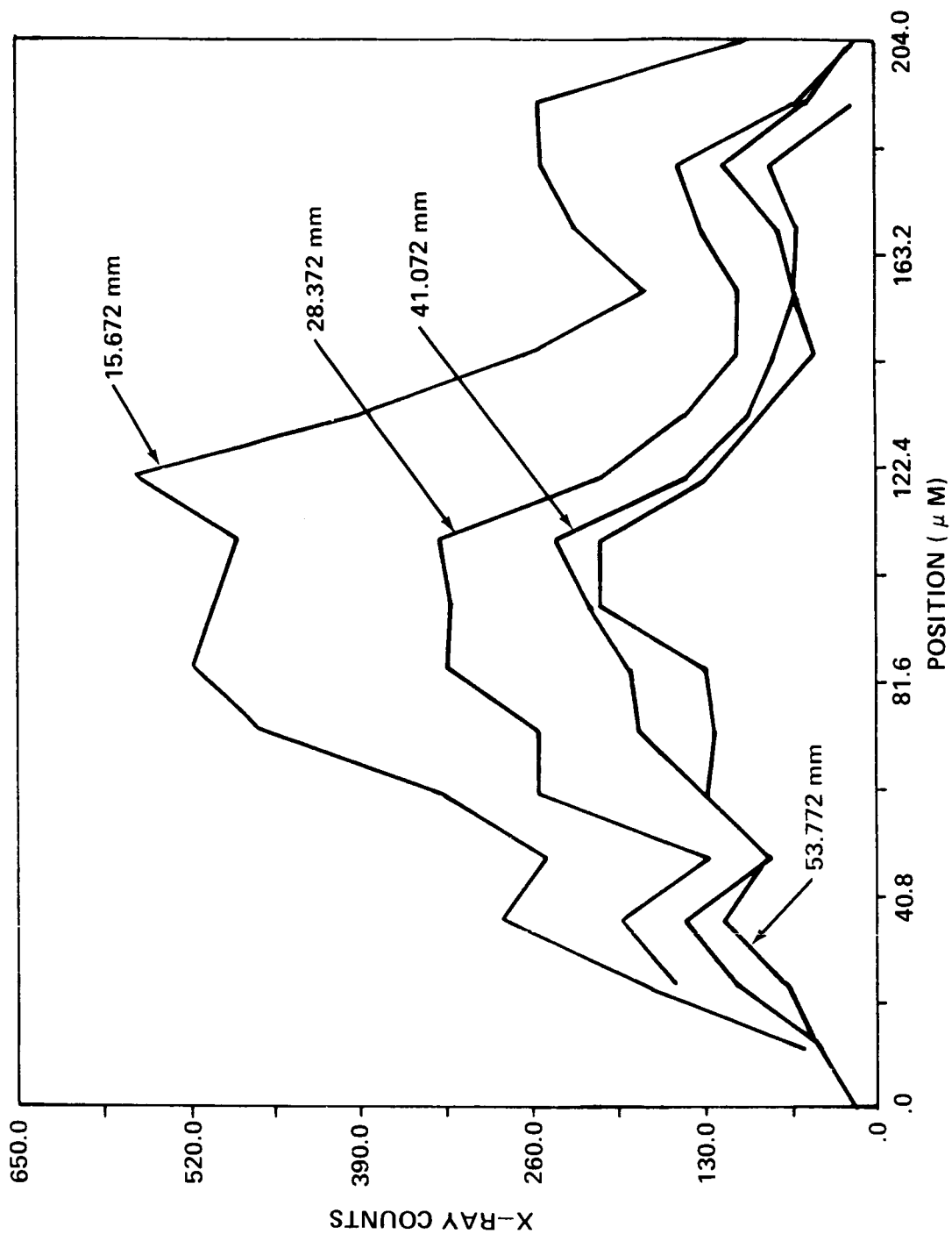


Figure 4. Radial profiles of ring annuli with 25 μm pinhole scan. Plot labels indicate distance in front of the best focus.

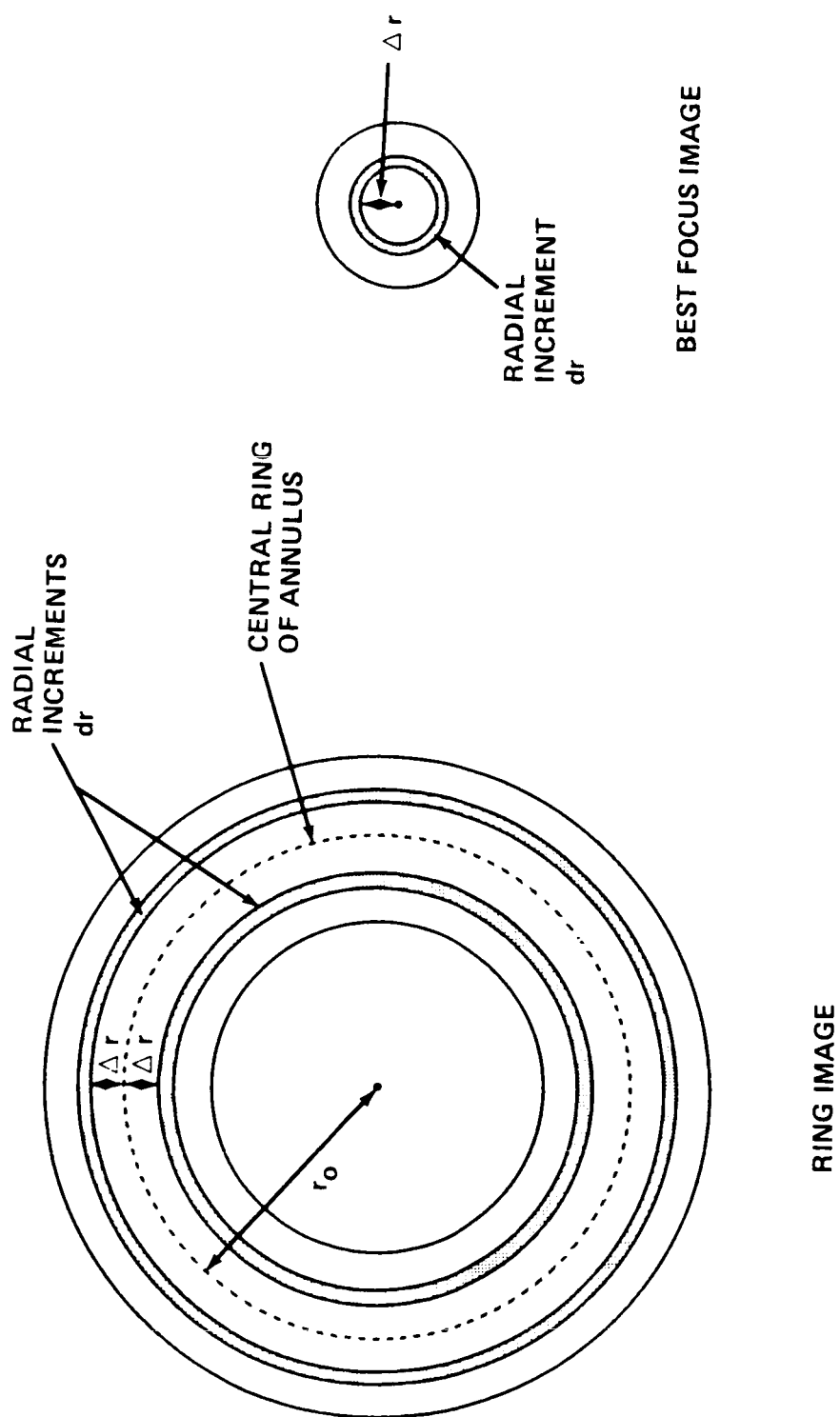


Figure 5. Variables used to describe correspondence between ring image and best focus image.

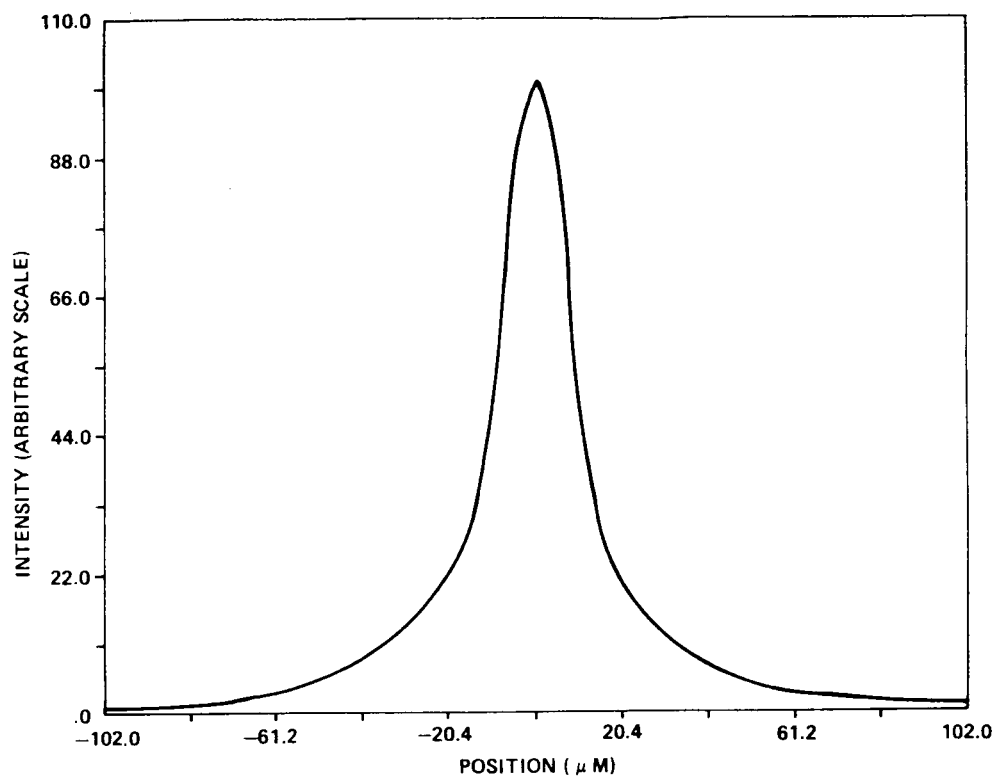


Figure 6. Parameterization of previously measured best focus image [4].

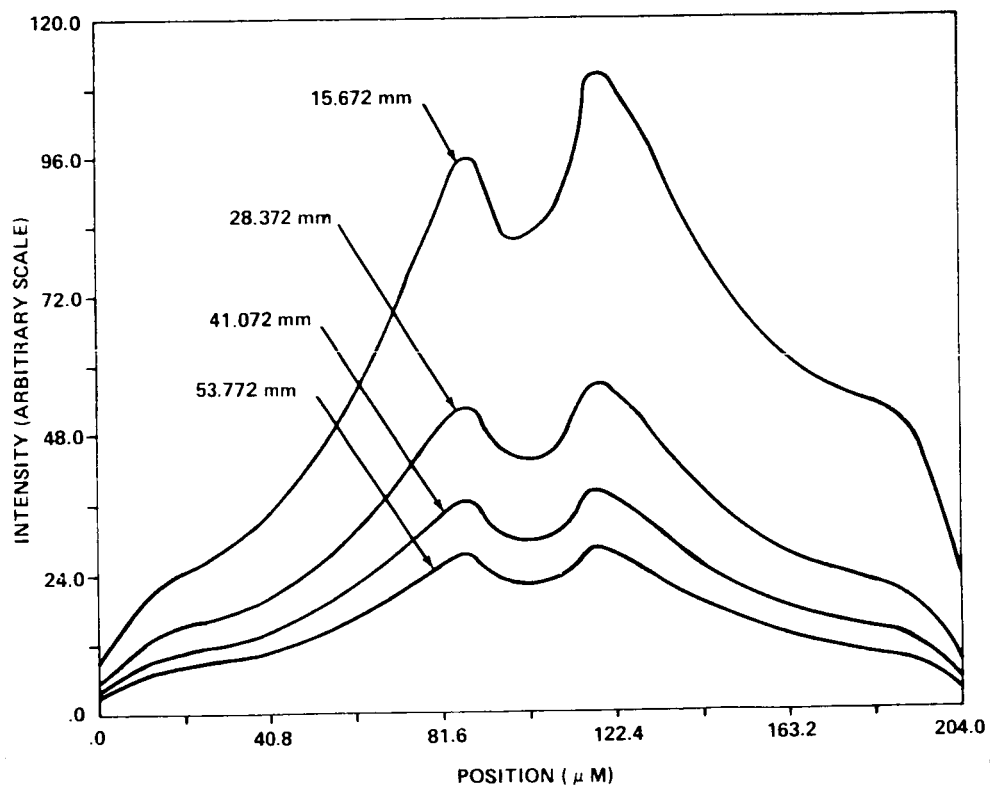


Figure 7. Model predictions from parameterized best focus data for radial profiles of ring annuli with a 25 μm pinhole scan. Plot labels indicate distance in front of the best focus.


APPROVAL

EXPERIMENTAL EVALUATION OF THE RING FOCUS TEST FOR X-RAY
TELESCOPES USING AXAF'S TECHNOLOGY MIRROR ASSEMBLY

MSFC Center Director's Discretionary Fund Final Report,
Project No. H20

By D. E. Zissa and D. Korsch

The information in this report has been reviewed for technical content. Review of any information concerning Department of Defense or nuclear energy activities or programs has been made by the MSFC Security Classification Officer. This report, in its entirety, has been determined to be unclassified.



W. C. BRADFORD
Director, Information and Electronic
Systems Laboratory